DMD Fast Forward. Published on August 26, 2020 as DOI: 10.1124/dmd.120.000188
This article has not been copyedited and formatted. The final version may differ from this version.

The Respective Roles of CYP3A4 and CYP2D6 in the Metabolism of Pimozide to Established and Novel Metabolites

Brian D. Chapron, Jean C. Dinh, Paul C. Toren, Andrea Gaedigk and J. Steven Leeder

Division of Clinical Pharmacology, Toxicology and Therapeutic Innovation, Department of Pediatrics (B.D.C., J.C.D., P.C.T., A.G. and J.S.L.), Children's Mercy Kansas City, Kansas City, Missouri, USA

Running title: Roles of CYP2D6 and CYP3A4 in pimozide metabolism

Corresponding author:

Brian D. Chapron

Division of Clinical Pharmacology, Toxicology and Therapeutic Innovation, Children's Mercy Kansas City, 2401 Gillham Rd, Kansas City, MO 64108.

Phone: +1-816-983-6508

Fax: +1-816-302-9943

Email: bchapron@cmh.edu

Number of text pages: 34

Number of tables: 3

Number of figures: 6

Number of references: 33

Number of words in the Abstract: 250

Number of words in the Introduction: 730

Number of words in the Discussion: 789

Non-standard abbreviations: CPIC, Clinical Pharmacogenetics Implementation Consortium; CYP, cytochrome P450; DHPBI, 1,3-dihydro-1-(4-piperidinyl)-2H-benzimidazol-2-one; DDI, drug-drug interaction; HLM, human liver microsome; MS/MS, tandem mass spectrometry; NM, normal metabolizer; PM, poor metabolizer; Q-TOF, quadrupole time-of-flight; SSRI, selective serotonin reuptake inhibitor; TS, Tourette Syndrome; UM, ultra rapid metabolizer; UPLC, ultra performance liquid chromatography.

DMD Fast Forward. Published on August 26, 2020 as DOI: 10.1124/dmd.120.000188
This article has not been copyedited and formatted. The final version may differ from this version.

Abstract

Pimozide is a dopamine receptor antagonist indicated for the treatment of Tourette syndrome. Prior *in vitro* studies characterized N-dealkylation of pimozide to 1,3-dihydro-1-(4-piperidinyl)-2H-benzimidazol-2-one (DHPBI) via CYP3A4, and to a lesser extent CYP1A2, as the only notable routes of pimozide biotransformation. However, drug-drug interactions between pimozide and CYP2D6 inhibitors, and *CYP2D6* genotype-dependent effects, have since been observed. To reconcile these incongruities between the prior *in vitro* and *in vivo* studies, we characterized two novel pimozide metabolites, 5-hydroxypimozide and 6-hydroxypimozide. Notably, 5-hydroxypimozide was the major metabolite produced by recombinant CYP2D6 (K_m ~82 nM, V_{max} ~0.78 pmol/min/pmol) and DHPBI was the major metabolite produced by recombinant CYP3A4 (apparent K_m ~1300 nM, V_{max} ~2.6 pmol/min/pmol). Kinetics in pooled human liver microsomes (HLMs) for the 5-hydroxylation (K_m ~ 2200 nM, V_{max} ~59 pmol/min/mg) and N-dealkylation (K_m ~3900 nM, V_{max} ~600 pmol/min/mg) reactions were also determined. Collectively, formation of DHPBI, 5-hydroxypimozide and 6-hydroxypimozide accounted for 90% of pimozide depleted in incubations of NADPH-supplemented pooled HLMs. Studies conducted in HLMs isolated from individual donors with specific CYP isoform protein abundances determined via mass spectrometry revealed that 5-hydroxypimozide (r^2=0.94) and 6-hydroxypimozide (r^2=0.86) formation rates were correlated with CYP2D6 abundance, whereas the DHPBI formation rate (r^2=0.98) was correlated with CYP3A4 abundance. Furthermore, the HLMs differed with respect to their capacity to form 5-hydroxypimozide relative to DHPBI. Collectively, these data confirm a role for CYP2D6 in pimozide clearance via 5-hydroxylation, and provide an explanation for a lack of involvement when only DHPBI formation was monitored in prior *in vitro* studies.

DMD Fast Forward. Published on August 26, 2020 as DOI: 10.1124/dmd.120.000188
This article has not been copyedited and formatted. The final version may differ from this version.

Significance Statement

Current *CYP2D6* genotype-guided dosing information in the pimozide label is discordant with available knowledge regarding the primary biotransformation pathways. Herein, we characterize the CYP2D6-dependent biotransformation of pimozide to previously unidentified metabolites. In human liver microsomes, formation rates for the novel metabolites and a previously identified metabolite were determined to be a function of CYP2D6 and CYP3A4 content, respectively. These findings provide a mechanistic basis for observations of *CYP2D6* genotype-dependent pimozide clearance *in vivo*.

Introduction

Tourette syndrome (TS) is a neuropsychiatric disorder that affects approximately 1% of children world-wide (Robertson, 2008). Two of the typical antipsychotics (pimozide and haloperidol) and a single atypical antipsychotic (aripiprazole) are the only drugs holding FDA-approved indications for the treatment of TS symptoms (Sallee et al., 2017). While these drugs appear to be comparably effective, both pimozide and aripiprazole elicit fewer extrapyramidal adverse effects than haloperidol (Shapiro et al., 1989; Sallee et al., 1997; Yoo et al., 2011). However, in the case of pimozide, clinical use remains limited due to concerns for potassium channel-dependent QTc prolongation (Haddad and Anderson, 2002; Gulisano et al., 2011; Beach et al., 2013).

While evidence suggests that the association between pimozide administration and QTc prolongation is concentration-dependent (Flockhart et al., 2000; Drolet et al., 2001), there are conflicting data regarding which clearance pathways meaningfully affect pimozide exposure. An early clinical study in a small set of subjects who were administered tritiated pimozide found that a N-dealkylation product of pimozide constituted the major source of radioactivity in the urine (Baro et al., 1972). Subsequent experiments in human liver microsomes (HLMs) further characterized 1,3-dihydro-1-(4-piperidinyl)-2H-benzimidazol-2-one (DHPBI), a N-dealkylation product of pimozide (Desta et al., 1998). Additional experiments applying cytochrome P450 (CYP) isoform-specific inhibitors to HLMs and using recombinant CYP expression systems demonstrated that the biotransformation of pimozide to DHPBI was principally mediated by CYP3A and, to a much lesser extent, by CYP1A2 (Desta et al., 1998). Interestingly, one study observed depletion of pimozide by recombinant CYP2D6 that was inhibitable by quinidine, a selective inhibitor of CYP2D6. However, DHPBI formation was not observed and the product of

the CYP2D6-mediated reaction was not reported (Flockhart, 1997). Subsequent experiments confirmed that quinidine co-incubation did not reduce DHPBI formation in HLMs (Desta et al., 1998).

In the 1990s, case reports of life-threatening and fatal interactions between pimozide and other drugs, notably clarithromycin and certain selective serotonin reuptake inhibitors (SSRIs) emerged (Ahmed et al., 1993; Horrigan and Barnhill, 1994; Flockhart, 1996; McIntyre et al., 1997). In response, clinical studies were conducted to better characterize the magnitude of the interactions with clarithromycin and the SSRIs, sertraline and paroxetine (Desta et al., 1999; Alderman, 2005; GlaxoSmithKline, 2008). While clarithromycin is known to be a potent inhibitor of CYP3A isoforms (Zhou et al., 2007), sertraline and paroxetine have traditionally been classified as inhibitors of CYP2D6 with a low potency for inhibiting CYP3A (Hemeryck and Belpaire, 2002). Nevertheless, all three drugs were observed to be capable of increasing pimozide exposure *in vivo*.

In 2007, a clinical study in adults demonstrated that the oral clearance of pimozide was 3-fold less in genotypic CYP2D6 poor metabolizers (PMs) compared to those genotyped as CYP2D6 normal metabolizers (NMs) (Nucci, 2007). The identification of a potential role for CYP2D6 in the metabolism of pimozide provided a basis for rationalizing how sertraline and paroxetine, both established CYP2D6 inhibitors, could result in alterations in pimozide oral clearance. While a proper explanation for the discrepancies between the *in vitro* and *in vivo* data remained absent, the FDA nevertheless requested changes to the pimozide product labeling to include a contraindication for the co-administration of strong CYP2D6 inhibitors (Rogers et al., 2012). Furthermore, multiple-dose simulations relying upon parameter estimates from the single-

dose clinical study were used to establish *CYP2D6* genotype-dependent dosing recommendations for pimozide in the FDA-approved labeling (Rogers et al., 2012).

In light of these changes in the pimozide labeling and the drug's narrow therapeutic index, it is crucial to reconcile the contrasting results from the *in vitro* and *in vivo* investigations of pimozide metabolism. As such, we have revisited the characterization of pimozide metabolism in HLMs and recombinant CYP expression systems. In the process, we have characterized two novel metabolites of pimozide that are preferentially produced by CYP2D6. Because the previous *in vitro* characterization of pimozide metabolism was conducted at exclusively supratherapeutic concentrations that might have underestimated the relative contribution of high-affinity low-capacity enzymes to overall metabolism *in vivo* (Desta et al., 1998), we have expressly designed our kinetic experiments to include therapeutically relevant pimozide concentrations (McCreadie et al., 1984). Through the use of HLMs isolated from individual donors with known CYP isoform abundances, we also evaluated the suitability of the formation of pimozide metabolites as potential probes of CYP2D6 and CYP3A4 function *in vitro*. The data suggest that CYP2D6-mediated biotransformation may represent a more dominant clearance pathway for pimozide than CYP3A4 in certain individuals.

Materials and Methods

Materials and Reagents. Pimozide was obtained from the United States Pharmacopeia (North Bethesda, MD). 5-hydroxypimozide and 6-hydropxypimozide were custom synthesized by Dalton Research Molecules (Toronto, Canada). Pimozide-d_5 and DHPBI-d_5 were purchased from Toronto Research Chemicals (North York, Canada). EasyCYP Bactosome recombinant human cytochrome P450 isoforms with co-expressed cytochrome P450 reductase and human liver microsomes were obtained from Sekisui XenoTech (Kansas City, KS). Magnesium chloride, DHPBI, NADPH, EDTA, potassium monophosphate and potassium diphosphate were obtained from Sigma Aldrich (St. Louis, MO). Analytical grade acetonitrile, methanol and formic acid were purchased from Thermo Fisher Scientific (Waltham, MA).

Metabolite Identification. Experiments to identify novel products of CYP2D6-mediated pimozide metabolism were conducted using recombinant human CYP2D6 with co-expressed cytochrome P450 reductase (Product #: CYP/EZ007) and HLMs from two individual donors (Product/lot #: H0033/0210015 and H0099/1110299) that were selected to represent the two extremes of *CYP2D6* genotype-predicted phenotype – a poor metabolizer (PM) (*CYP2D6*4/*5*) and an ultra rapid metabolizer (UM) (*CYP2D6*1/*2x2*). The *CYP2D6* genotype for each of the HLM donors was provided by the supplier, Sekisui XenoTech. Each of these exploratory experiments were performed once in technical duplicate and deviated from the general incubation protocol that was subsequently optimized for the quantitative experiments. Recombinant CYP2D6 Bactosomes (10 pmol/mL, 250 µL incubation volume) with co-expressed cytochrome P450 reductase and HLMs (500 µg/mL, 250 µL incubation volume) were each pre-incubated for 5 min at 37°C in 100 mM potassium phosphate buffer (pH~7.4) containing the

following pimozide concentrations: 0, 25, 50, 100, 1000 and 10000 nM. Reactions were initiated with 1 mM NADPH and quenched after 30 min with 125 µL of ice-cold methanol containing internal standards (100 nM pimozide-d_5 and DHPBI-d_5). Samples were centrifuged at 16.3 *g* for 10 min. Supernatant was collected and applied to an Acquity UPLC BEH C18 1.7 µm, 2.1 x 100 mm column on an Acquity M-Class UPLC in tandem with a XEVO G2-XS quadrupole time-of-flight (Q-TOF) mass spectrometer (Waters Corporation, Milford, MA). The typical limit of detection for analytes on this instrument is 1 to 10 nM. The aqueous mobile phase consisted of 0.1% formic acid in water (solvent A) and the organic mobile phase consisted of 0.1% formic acid in acetonitrile (solvent B). The UPLC mobile gradient used is as follows: initial conditions of solvent were 1% solvent B held for 0.2 min; the percent of solvent B increased linearly to 99% at 6 min and was held until 7 min. Q-TOF data was assessed, in particular comparing the metabolite profile from the *CYP2D6* PM and the UM incubated with 10000 nM pimozide. Daughter fragmentation was assessed for pimozide and two putative metabolites with the same column and solvent gradient on a XEVO-TQD (Waters Corporation, Milford, MA); further details for the assay conditions are provided in the supplemental information (Supplemental Table 1). SmartCYP software was then used to determine the most likely locations for CYP2D6-dependent oxidation of pimozide (Rydberg et al., 2010). Once standards for the suspected metabolites were synthesized, further incubations were conducted to identify the major site of metabolism by CYP2D6 and to confirm prior observations that DHPBI is the major metabolite of pimozide produced by CYP3A4. These follow-up incubations were conducted in singlet and used 10 nM (a nominally therapeutic concentration) of pimozide and 2 mL of 2 pmol/mL recombinant human CYP2D6 and CYP3A4. The incubations were quenched 8 min after initiation with NADPH and adhered to the general incubation conditions. These samples were

analyzed according to the XEVO TQ-XS UPLC-M/MS method described below and a comparison of retention times and mass transitions was made to chromatograms from standards of DHPBI, 5-hydroxypimozide and 6-hydroxypimozide.

Quantitative UPLC-MS/MS Analysis. Samples and calibration curve standards were centrifuged at 16.3 *g* for 5 min to pellet protein. Subsequently, 100 µL of supernatant were transferred to glass vials containing 400 µL deionized water. Analytes were quantified via ultra performance liquid chromatography (UPLC) and tandem mass spectrometry (MS/MS) on an Acquity UPLC I-Class coupled to a Xevo TQ-XS triple quadrupole mass spectrometer (Waters Corporation, Milford, MA) equipped with an electrospray ionization source. Chromatographic separation of DHPBI, 5-hydroxypimozide, 6-hydroxypimozide and pimozide was achieved on a Waters Acquity BEH C18, 1.7 µm x 2.1 mm x 100 mm column heated to 60ºC. Mobile phase A (aqueous) consisted of 0.1% formic acid in water and mobile phase B (organic) consisted of 0.1% formic acid in acetonitrile. An initial flow rate of 0.4 mL/min of 95% phase A and 5% phase B was used. From 0.25 to 2 min, a linear gradient increasing the proportion of phase B to 25% was established, followed by a brief linear gradient to 30% phase B at 2.05 min. Proportion of phase B further increased along a linear gradient to 35% at 5 min and then along another linear gradient to 40% at 7 min. The column was then washed with 98% of phase B at 0.5 mL/min and equilibrated to initial conditions prior to the next sample injection. The mass spectrometer was operated in positive ion mode and multiple reaction monitoring was employed. The mass transitions for the analytes were as follows: DHPBI was *m/z* 218.10→84.00, DHPBI-d_5 was *m/z* 223.10→89.00, pimozide was *m/z* 462.30→328.10, pimozide-d_5 was *m/z* 467.30→333.10, 5-hydroxypimozide and 6-hydroxypimozide were *m/z* 478.30→328.10. Further

details for the assay conditions are provided in the supplemental information (Supplemental Table 2). Standard curves were used in the estimation of analyte concentrations and specific ranges are listed within respective methods sections. Peak areas were integrated, and sample concentrations were estimated in TargetLynx software version 4.2. (Waters Corporation, Milford, MA).

General Incubation Conditions. Incubations were conducted in 50 mM potassium phosphate buffer containing 5 mM magnesium chloride, 1 mM EDTA and either purified recombinant cytochrome P450s (EasyCYP Bactosomes) or HLMs. Protein and substrate (pimozide) concentrations varied depending upon the specific experiment but acetonitrile, the vehicle for pimozide, was limited to 0.5% v/v during all incubations. Following a 5-minute pre-incubation step to equilibrate reactions to 37°C, experiments were initiated with the addition of NADPH (1 mM final concentration). Parallel incubations without NADPH were used as negative controls with the exception of the recombinant CYP panel that used Bactosomes prepared from a blank vector as a control. Duration of incubations varied across the sets of experiments. Reactions were quenched with 2-fold greater volume of ice-cold acetonitrile containing 40 nM DHPBI-d_5 (internal standard for DHPBI) and 400 nM pimozide-d_5 (internal standard for pimozide, 5-hydroxypimozide and 6-hydroxypimozide). Any deviations from these general incubation conditions for any experiments are described in the relevant methods sections.

Molar Balance in Pooled HLMs. Using the general incubation conditions, 200 µL of 200 µg/mL pooled HLMs (200 donors, 50% female, product/lot #: H2620/1910096) were incubated with 50 nM pimozide for 20 min. These conditions were not linear with respect to time. The

experiment was repeated in triplicate with technical duplicates. Concentrations of DHPBI, pimozide, 5-hydroxypimozide and 6-hydroxypimozide were determined in the samples and compared to concentrations of pimozide in the incubation buffer at time 0 that were proportionally diluted with buffer absent of NADPH. Concentrations of analytes were determined via the quantitative UPLC-MS/MS assay using calibration curves ranging from 0.25 to 50 nM for 5-/6-hydroxypimozide and 1 to 50 nM DHPBI. In order to estimate substrate depletion, pimozide concentrations (calibration curve 5 to 500 nM) were also determined for this experiment. Analyte concentrations were converted to molar amounts and the percentage of NADPH-dependent pimozide loss over the course of the incubation was calculated using Equation 1.

$$\%\, Accounted = \frac{DHPBI_{t=20} + 5OHPIM_{t=20} + 6OHPIM_{t=20}}{PIM_{t=0} - PIM_{t=20}} \quad (1)$$

Wherein the amounts of DHPBI, 5-hydroxpimozide, 6-hydroxypimozide and pimozide measured at 20 min are represented by the parameters $DHPBI_{t=20}$, $5OHPIM_{t=20}$, $6OHPIM_{t=20}$ and $PIM_{t=20}$ respectively. The starting amount of pimozide is represented by the $PIM_{t=0}$ parameter.

Panel of Recombinant CYP Isoforms. The capacity to catalyze the formation of DHPBI, 5-hydroxypimozide and 6-hydroxypimozide from pimozide (2500 nM) was evaluated in purified recombinant CYP enzymes with co-expressed CYP reductase, and some co-expressing cytochrome b_5, for the following 14 known drug-metabolizing isoforms (EasyCYP Bactosome product numbers provided in parentheses): CYP1A1 (CYP/EZ018), CYP1A2 (CYP/EZ012), CYP2A6 (CYP/EZ011), CYP2B6 (CYP/EZ016), CYP2C8 (CYP/EZ047), CYP2C9 + b_5

(CYP/EZ038), CYP2C18 (CYP/EZ022), CYP2C19 (CYP/EZ028), CYP2D6 (CYP/EZ013), CYP2E1 + b_5 (CYP/EZ036), CYP2J2 (CYP/EZ034), CYP3A4 + b_5 (CYP/EZ035), CYP3A5 + b_5 (CYP/EZ045) and CYP3A7 + b_5 (CYP/EZ060). The general incubation conditions were followed. All CYP isoforms were evaluated at a protein concentration of 2 pmol/mL (final incubation volume = 200 µL) and Bactosomes prepared from a blank vector were used as a control. Incubations were quenched at 30 min following initiation with NADPH. These conditions were not confirmed to be linear with respect to time. The experiment was repeated in triplicate with technical singlets. Concentrations of analytes were determined via the quantitative UPLC-MS/MS assay using calibration curves with the following quantitative ranges: 1 to 250 nM for 5-/6-hydroxypimozide and 5 to 250 nM for DHPBI.

Enzyme Kinetics. Under the general incubation conditions, EasyCYP Bactosomes for CYP2D6 (product #: CYP/EZ013) and CYP3A4 (product #: CYP/EZ035) were incubated at cytochrome P450 protein concentrations of 1 pmol/mL and 2 pmol/mL respectively. Kinetic experiments using HLMs pooled from 200 donors (50% female, product/lot #: H2620/1910096) were conducted at protein concentration of 50 µg/mL. A range of pimozide concentrations for CYP2D6 Bactosomes (10 to 2500 nM), CYP3A4 Bactosomes (10 to 5000 nM) and pooled HLMs (25 to 10000 nM) were selected in order to span both nominally therapeutic and enzyme-saturating substrate concentrations. Final incubation volumes were 400 µL for recombinant expression systems and 200 µL for pooled HLMs. The durations of the incubations were 5 min for both pooled HLMs and CYP2D6 Bactosomes, and 20 min for CYP3A4 following reaction initiation. These conditions were determined to be linear with respect to time. Parallel incubations without NADPH were used as negative controls. Samples were analyzed via UPLC-

MS/MS using calibration curves that ranged from 0.25 to 500 nM for both 5-/6-hydroxypimozide and DHPBI. A single-enzyme Michaelis-Menten model was fit to the 5-hydroxypimozide and DHPBI formation rate data using GraphPad Prism version 8.1.2. (GraphPad Software, San Diego, CA). These experiments were conducted in triplicate with technical duplicates. Estimates for of K_m and V_{max} were determined for each replicate experiment and the mean and SD of these point estimates was calculated.

Pimozide Metabolite Formation in HLMs from Individual Donors. Protein expression of CYP2D6 and CYP3A4 in commercially acquired HLMs from 7 separate donors was determined by Dr. Bhagwat Prasad (University of Washington, now Washington State University) via MS/MS according to a protocol established by his group (Vrana et al., 2017; Bhatt et al., 2018; Bhatt and Prasad, 2018). All donors were Caucasian and genotyped; none carried the *CYP3A7*1C* allele. Genotype information for *CYP2D6* was provided by the HLM supplier, Sekisui XenoTech, and activity scores were assigned according to the Clinical Pharmacogenetics Implementation Consortium (CPIC) guidelines (Caudle et al., 2020). Tissue donor demographics, *CYP2D6* genotypes, specific CYP protein content and relevant product/lot numbers of the HLMs are summarized in Table 1. Under the general incubation conditions, 200 µL of 200 µg/mL of HLMs from the separate donors were each incubated for 5 min with 5 µM pimozide. These incubation conditions were determined to be linear with respect to time. The experiment was repeated in triplicate with technical duplicates. Parallel incubations without NADPH were used as negative controls. Concentrations of metabolites were determined via UPLC-MS/MS using calibration curves ranging from 0.5 to 500 nM for 5-/6-hydroxypimozide and 1 to 500 nM for DHPBI. A simple linear regression model was fit to 5-/6-hydroxypimozide

metabolite and DHPBI formation rate data and expression of CYP2D6 and CYP3A4 protein using Graphpad Prism software version 8.1.2. (San Diego, CA). As expected, the HLMs prepared from the single *CYP2D6* PM (**4/*5* genotype) donor did not have detectable levels of CYP2D6 protein and was thus assigned an abundance of 0 pmol/mg microsomal protein. The formation rates for "gold-standard" phenotyping reactions for CYP2D6 (dextromethorphan *O*-demethylation) and CYP3A4 (midazolam 1'-hydroxylation and testosterone 6β-hydroxylation) were provided by the supplier (Sekisui XenoTech, Kansas City, KS) for the HLMs from each of the donors. For purposes of comparison, a linear regression model was also fit to this vendor-supplied data. However, it should be noted that the exact protocol for the manufacturer-supplied phenotyping reactions is unknown and should be interpreted with caution.

Results

Prediction and Identification of the Product of CYP2D6-Mediated Metabolism of Pimozide. The Q-TOF analysis of metabolite profiles from the exploratory incubations of pimozide in recombinant CYP2D6 and HLMs from a *CYP2D6* UM revealed a metabolite that was consistent with hydroxylation (i.e. +16 Da). This peak was not present in the incubation using HLMs isolated from a *CYP2D6* PM. The fragmentation pattern of the +16 Da metabolite produced by incubating 10 μM pimozide in *CYP2D6* UM HLM incubations was analyzed on a XEVO-TQD mass spectrometer and suggested that oxidation occurred on the benzimidazolone moiety of the pimozide molecule; the major fragment (daughter ion *m/z* 328) from both pimozide and hydroxypimozide molecules occurred between the piperidine ring and benzimidazolone moiety (Supplemental Figure 1). SmartCYP software was used to determine the most likely sites for CYP2D6-mediated oxidation of pimozide. It assigned the greatest likelihood to the 5 position on the aromatic ring of the benzimidazolone moiety; the adjacent 6 position was determined to be the second most likely site of CYP2D6-mediated metabolism (Supplemental Figure 2). When recombinant CYP2D6 was incubated with a therapeutically relevant concentration of pimozide (10 nM) and the incubation product was analyzed via UPLC-MS/MS, peaks with the same *m/z* transition and corresponding elution times to NMR-validated standards for 5- and 6-hydroxypimozide were observed (Figure 1). The peak height and area were larger for 5-hydroxypimozide than 6-hydroxypimozide. It is important to note that 4- or 7-hydroxypimozide could theoretically co-elute with 5-hydroxypimozide under the chromatographic conditions used. Therefore, the absence of authentic standards for the products of the less likely 4- and 7-hydroxylation reactions preclude definitive confirmation that 5-hydroxypimozide is the major metabolite produced by CYP2D6. When recombinant CYP3A4 was incubated with pimozide under otherwise identical incubation conditions, a peak corresponding to the same *m/z* transition

and elution time as a commercially available authentic standard for DHPBI was observed (Figure 1). It is worth noting that CYP3A4 did not produce detectable amounts of either of the hydroxylated pimozide metabolites under these therapeutically relevant conditions. However, when recombinant CYP3A4 was incubated with substantially greater pimozide concentrations as part of subsequent kinetic studies (described in the "Kinetics of Pimozide Metabolism" methods section), detectable formation of both hydroxylated metabolites was observed. Relative to CYP2D6, recombinant CYP3A4 was less selective for the production of one hydroxypimozide isomer over the other (Supplemental Figure 3).

Molar Balance of Pimozide Metabolism in Pooled HLMs. The NADPH-dependent conversion of pimozide to DHPBI, 5-hydroxypimozide and 6-hydroxypimozide was evaluated in pooled HLMs. The most abundant metabolite formed was DHPBI, followed by 5-hydroxypimozide and then 6-hydroxypimozide (Table 2). According to Equation 1, 90% of the pimozide that was depleted over the course of the experiment could collectively be accounted for by these three pimozide metabolites. The conditions used in this experiment are non-linear with respect to time and caution is advised regarding any kinetic interpretation of the data.

Recombinant P450 Screen. CYP2D6 was the predominate isoform to produce 5- and 6-hydroxypimozide and favored the production of 5-hydroxypimozide over 6-hydroxypimozide (Table 3). However, other CYP isoforms including CYP1A1, CYP1A2, CYP2C18, CYP2J2, CYP3A4, CYP3A5 and CYP3A7 also catalyzed the formation of lesser amounts of the hydroxypimozide isomers. Only CYP3A isoforms formed detectable amounts of DHPBI; CYP3A4 was the most active of the CYP3A isoforms.

DMD Fast Forward. Published on August 26, 2020 as DOI: 10.1124/dmd.120.000188
This article has not been copyedited and formatted. The final version may differ from this version.

Kinetics of Pimozide Metabolism. Experiments evaluating the kinetics of pimozide biotransformation via CYP2D6 and CYP3A4 to their principle metabolite products, 5-hydroxypimozide and DHPBI respectively, were conducted in recombinant human CYPs and pooled HLMs. Formation rates were plotted against substrate (i.e. pimozide) concentrations and a simple single-enzyme Michaelis-Menten model was fit to the data. A representative Michaelis-Menten curve and estimates for K_m and V_{max} for the recombinant enzymes and pooled HLMs are presented in Figure 2 and Figure 3 respectively. The K_m and V_{max} for DHPBI formation in CYP3A4 Bactosomes were respectively 15- and 3-fold greater than 5-hydroxypimozide formation in CYP2D6 Bactosomes. However, when subsequent incubations were conducted in pooled HLMs, the differences in affinity for the principally CYP3A4-mediated N-dealkylation reaction (K_m ~ 3900 nM) and the principally CYP2D6-mediated 5-hydroxylation reaction (K_m ~ 2200 nM) were less pronounced. The V_{max} for the N-dealkylation reaction (~600 pmol/min/mg protein) was greater than that of the 5-hydroxylation reaction (~59 pmol/min/mg protein) in pooled HLMs.

Pimozide Metabolite Formation Correlates with Protein Abundance of CYP2D6 and CYP3A4 in HLMs. Both pimozide 5-hydroxylation (r^2 = 0.94) and 6-hydroxylation (r^2 = 0.86) rates were positively linearly correlated with abundance of CYP2D6 protein (Figure 4). Notably, the correlation between the vendor-supplied rate of dextromethorphan *O*-demethylation to dextrorphan and CYP2D6 protein abundance (r^2 = 0.93) was comparable to that of 5-hydroxypimozide (Supplemental Figure 4). There was poor linear correlation between either pimozide 5-hydroxylation (r^2 = 0.08) or 6-hydroxylation (r^2 = 0.26) rates and CYP3A4

abundance (Supplemental Figure 5). Expression levels of CYP2D6 protein and formation rates for 5-hydroxypimozide and 6-hydroxypimozide were observed generally to be greater in individuals with a higher activity score assignment. However, there was overlap between the 1.0 (green) and 2.0 (blue) *CYP2D6* activity score groups (Figure 4). The DHPBI formation rate was positively correlated with abundance of CYP3A4 protein (r^2 = 0.98) (Figure 5). For comparison, a simple linear regression model fit the vendor-supplied rates for either testosterone 6β-hydroxylation or midazolam 1'-hydroxylation and CYP3A4 protein abundance yielded r^2 values of 0.77 and 0.39 respectively (Supplemental Figure 6). There was poor linear correlation (r^2 = 0.12) between DHPBI formation rate and CYP2D6 abundance (Supplemental Figure 7).

Discussion

Initial clinical studies observed that pimozide was primarily excreted in the form of N-dealkylation products in the urine (Baro et al., 1972; Pinder et al., 1976). Ensuing *in vitro* investigations focused solely on N-dealkylation to DHPBI (Desta et al., 1998; Desta et al., 2002), establishing DHPBI formation as the primary route of pimozide metabolism and identifying CYP3A4 (and to a much lesser extent CYP1A2) as the mediating enzymes (Desta et al., 1998). However, subsequent *in vivo* studies demonstrated that *CYP2D6* genotype and the co-administration of CYP2D6 inhibitors have an effect on pimozide exposure (Alderman, 2005; Nucci, 2007; GlaxoSmithKline, 2008). The findings described herein present a plausible case for reconciling the discordance between the previously published *in vitro* and *in vivo* studies. We have identified two novel metabolites of pimozide, 5- and 6-hydroxypimozide (Figure 1), and determined that both metabolites, but particularly 5-hydroxypimozide, are formed via CYP2D6 (Table 3). This finding, in conjunction with confirmation of previous observations of negligible DHPBI formation by CYP2D6 (Desta et al., 1998), suggests that assessment of N-dealkylation rate is not the most appropriate means to evaluate the contribution of CYP2D6 to pimozide biotransformation. Furthermore, our experiments comparing the kinetics of pimozide metabolism to 5-hydroxypimozide and DHPBI by CYP2D6 and CYP3A4 respectively, suggest that CYP2D6 represents a moderately higher affinity (i.e. lower K_m) pathway (Figures 2 and 3).

Collectively, the three metabolites monitored in our experiments (DHPBI, 5-hydroxypimozide and 6-hydroxypimozide) account for 90% of the products of NADPH-dependent biotransformation in pooled HLMs, strongly suggesting that we are capturing a near-complete picture of the extent of NADPH-dependent pimozide metabolism occurring in HLMs (Table 2). While DHPBI represented the major metabolite formed by pooled HLMs (n = 200 donors) (Figure 3), we observed that the relative rates of production for the three metabolites

varied across HLMs sourced from individual donors and was dependent upon the underlying abundance of CYP2D6 (Figure 4) and CYP3A4 (Figure 5) protein in the microsomes. Interestingly, in HLMs from two of the seven individual donors evaluated, the pimozide 5-hydroxylation rate exceeded the N-dealkylation rate, suggesting that CYP2D6 may be the major route of metabolism in those individuals. Notably, CYP2D6 and CYP3A4 protein expression did not correlate with each other (Supplemental Figure 8). One limitation of these experiments was that none of the HLMs expressed CYP3A7 (no neonatal/fetal donors or adults possessing the *CYP3A7*1C* functional adult expresser allele). Despite observations of pimozide N-dealkylation by recombinant CYP3A7 (Table 3), we were unable to evaluate the contribution of hepatic CYP3A7 abundance on pimozide N-dealkylation.

Collectively, these observations warrant a revised pathway for pimozide biotransformation (Figure 6), with the understanding that the major pathway of systemic metabolism will be dependent on the relative degree of hepatic CYP2D6 and CYP3A4 activity in a given individual. Individual expression levels of CYP2D6 and CYP3A4 would also be anticipated to impact the magnitude of pharmacokinetic drug-drug interactions (DDIs) between pimozide and inhibitors of these enzymes (i.e. DDI sensitivity); the effects could range from negligible to profound depending on the relative fractional clearance via each of these enzymatic pathways. In light of this, the utilization of pathway-specific metabolites may provide a means for predicting individualized dosing and DDI sensitivity. The strong correlations we observed between the formation of the different pimozide metabolites and the expression of the respective enzymes that mediate their production is encouraging. In the future, DHPBI and 5-hydroxypimozide levels in the blood or urine may have utility in the prediction of the relative sensitivity for CYP2D6- versus CYP3A4-dependent DDIs with pimozide for a given individual.

Additional studies will need to be conducted to determine the extent to which 5-hydroxypimozide is produced *in vivo* and present in the blood and excreta. While the pharmacologic activity of 5-hydroxypimozide is unknown, it may also be necessary to characterize its activity profile if the metabolite is found to circulate *in vivo*. Interestingly, human clinical trials evaluating the effectiveness of 5-chloropimozide, an analogue of pimozide that was ultimately never marketed, demonstrated the investigational drug to be a "highly potent" and "long acting" dopamine receptor antagonist (Janssen et al., 1975), thus suggesting that 5-hydroxypimozide may retain pharmacologic activity.

In conclusion, our discovery of CYP2D6-mediated metabolism of pimozide to 5- and 6-hydroxypimozide illuminates a longstanding knowledge deficit in our understanding of the drug's *in vivo* disposition. Our findings provide a mechanistic basis for prior clinical observations of reduced pimozide oral clearance in individuals who are *CYP2D6* PMs or who are concomitantly taking certain CYP2D6 inhibitors (e.g. paroxetine and sertraline) (Alderman, 2005; Nucci, 2007; GlaxoSmithKline, 2008). Application of the approach we have used may prove useful in the reassessment of other drugs. As with pimozide, identification of novel metabolites could be required and modern *in silico* tools such as SmartCYP may provide useful guidance in the process.

Acknowledgements

We would like to thank Dr. Leon Van Haandel, Dr. Annemarie Rompca, and Dr. Robin Pearce for their technical assistance. We would also like to thank Kim Gibson and Dr. Whitney Nolte for their assistance with the maintenance and operation of analytical instrumentation.

Authorship contributions

Participated in research design: Chapron, Dinh, Leeder

Conducted experiments: Chapron, Dinh, Toren, Gaedigk

Contributed new reagents or analytic tools: Leeder, Gaedigk

Performed data analysis: Chapron, Toren, Dinh, Gaedigk

Wrote or contributed to the writing of the manuscript: Chapron, Leeder, Gaedigk, Dinh

References

Ahmed I, Dagincourt PG, Miller LG, and Shader RI (1993) Possible interaction between fluoxetine and pimozide causing sinus bradycardia. *Canadian journal of psychiatry Revue canadienne de psychiatrie* **38:**62-63.

Alderman J (2005) Coadministration of sertraline with cisapride or pimozide: an open-label, nonrandomized examination of pharmacokinetics and corrected QT intervals in healthy adult volunteers. *Clinical therapeutics* **27:**1050-1063.

Baro F, Brugmans J, and Heykants J (1972) [Absorption, metabolism and excretion of pimozide in man]. *La Clinica terapeutica* **63:**239-249.

Beach SR, Celano CM, Noseworthy PA, Januzzi JL, and Huffman JC (2013) QTc prolongation, torsades de pointes, and psychotropic medications. *Psychosomatics* **54:**1-13.

Bhatt DK, Basit A, Zhang H, Gaedigk A, Lee SB, Claw KG, Mehrotra A, Chaudhry AS, Pearce RE, Gaedigk R, Broeckel U, Thornton TA, Nickerson DA, Schuetz EG, Amory JK, Leeder JS, and Prasad B (2018) Hepatic Abundance and Activity of Androgen- and Drug-Metabolizing Enzyme UGT2B17 Are Associated with Genotype, Age, and Sex. *Drug metabolism and disposition: the biological fate of chemicals* **46:**888-896.

Bhatt DK and Prasad B (2018) Critical Issues and Optimized Practices in Quantification of Protein Abundance Level to Determine Interindividual Variability in DMET Proteins by LC-MS/MS Proteomics. *Clin Pharmacol Ther* **103:**619-630.

Caudle KE, Sangkuhl K, Whirl-Carrillo M, Swen JJ, Haidar CE, Klein TE, Gammal RS, Relling MV, Scott SA, Hertz DL, Guchelaar HJ, and Gaedigk A (2020) Standardizing CYP2D6 Genotype to Phenotype Translation: Consensus Recommendations from the Clinical

Pharmacogenetics Implementation Consortium and Dutch Pharmacogenetics Working Group. *Clinical and translational science* **13:**116-124.

Desta Z, Kerbusch T, and Flockhart DA (1999) Effect of clarithromycin on the pharmacokinetics and pharmacodynamics of pimozide in healthy poor and extensive metabolizers of cytochrome P450 2D6 (CYP2D6). *Clin Pharmacol Ther* **65:**10-20.

Desta Z, Kerbusch T, Soukhova N, Richard E, Ko JW, and Flockhart DA (1998) Identification and characterization of human cytochrome P450 isoforms interacting with pimozide. *The Journal of pharmacology and experimental therapeutics* **285:**428-437.

Desta Z, Soukhova N, and Flockhart DA (2002) In vitro inhibition of pimozide N-dealkylation by selective serotonin reuptake inhibitors and azithromycin. *Journal of clinical psychopharmacology* **22:**162-168.

Drolet B, Rousseau G, Daleau P, Cardinal R, Simard C, and Turgeon J (2001) Pimozide (Orap) prolongs cardiac repolarization by blocking the rapid component of the delayed rectifier potassium current in native cardiac myocytes. *Journal of cardiovascular pharmacology and therapeutics* **6:**255-260.

Flockhart DA, Drici MD, Kerbusch T, Soukhova N, Richard E, Pearle PL, Mahal SK, and Babb VJ (2000) Studies on the mechanism of a fatal clarithromycin-pimozide interaction in a patient with Tourette syndrome. *Journal of clinical psychopharmacology* **20:**317-324.

Flockhart DAR, E.; Soukova, N.; Kerbuscb, T. (1997) Metabolism of pimozide by CYF3A and CYP2D6 in human liver microsomes. *Clinical Pharmacol Ther* **61:**232.

Flockhart DAR, E.; Woosley, R.L.; Pearle, P.L.; Drici, M.D. (1996) A Metabolic Interaction Between Clarithromycin and Pimozide May Result in Cardiac Toxicity. *Clin Pharmacol Ther* **59:**189.

GlaxoSmithKline (2008) Paxil Prescribing Information, United States Food and Drug Administration, https://http://www.accessdata.fda.gov/drugsatfda_docs/label/2009/020031s05920710s023lbl.pdf.

Gulisano M, Cali PV, Cavanna AE, Eddy C, Rickards H, and Rizzo R (2011) Cardiovascular safety of aripiprazole and pimozide in young patients with Tourette syndrome. *Neurological sciences : official journal of the Italian Neurological Society and of the Italian Society of Clinical Neurophysiology* **32:**1213-1217.

Haddad PM and Anderson IM (2002) Antipsychotic-related QTc prolongation, torsade de pointes and sudden death. *Drugs* **62:**1649-1671.

Hemeryck A and Belpaire FM (2002) Selective serotonin reuptake inhibitors and cytochrome P-450 mediated drug-drug interactions: an update. *Current drug metabolism* **3:**13-37.

Horrigan JP and Barnhill LJ (1994) Paroxetine-pimozide drug interaction. *Journal of the American Academy of Child and Adolescent Psychiatry* **33:**1060-1061.

Janssen PA, Niemegeers CJ, Schellekens KH, Lenaerts FM, and Wauquier A (1975) Clopimozide (R 29 764), a new highly potent and orally long-acting neuroleptic of the diphenylbutylpiperidine series. *Arzneimittel-Forschung* **25:**1287-1294.

McCreadie RG, Mackie M, Wiles DH, Jorgensen A, Hansen V, and Menzies C (1984) Within-individual variation in steady state plasma levels of different neuroleptics and prolactin. *The British journal of psychiatry : the journal of mental science* **144:**625-629.

McIntyre IM, King CV, Staikos V, Gall J, and Drummer OH (1997) A fatality involving moclobemide, sertraline, and pimozide. *Journal of forensic sciences* **42:**951-953.

Nucci GM, K.; Gomeni, R (2007) Population pharmacokinetic modelling of pimozide and its relation to CYP2D6 genotype, in: *Annual Meeting of Population Approach Group in Europe*, Copenhagen, Denmark.

Pinder RM, Brogden RN, Swayer R, Speight TM, Spencer R, and Avery GS (1976) Pimozide: a review of its pharmacological properties and therapeutic uses in psychiatry. *Drugs* **12:**1-40.

Robertson MM (2008) The prevalence and epidemiology of Gilles de la Tourette syndrome. Part 1: the epidemiological and prevalence studies. *Journal of psychosomatic research* **65:**461-472.

Rogers HL, Bhattaram A, Zineh I, Gobburu J, Mathis M, Laughren TP, and Pacanowski M (2012) CYP2D6 genotype information to guide pimozide treatment in adult and pediatric patients: basis for the U.S. Food and Drug Administration's new dosing recommendations. *The Journal of clinical psychiatry* **73:**1187-1190.

Rydberg P, Gloriam DE, and Olsen L (2010) The SMARTCyp cytochrome P450 metabolism prediction server. *Bioinformatics (Oxford, England)* **26:**2988-2989.

Sallee F, Kohegyi E, Zhao J, McQuade R, Cox K, Sanchez R, van Beek A, Nyilas M, Carson W, and Kurlan R (2017) Randomized, Double-Blind, Placebo-Controlled Trial Demonstrates the Efficacy and Safety of Oral Aripiprazole for the Treatment of Tourette's Disorder in Children and Adolescents. *Journal of child and adolescent psychopharmacology* **27:**771-781.

Sallee FR, Nesbitt L, Jackson C, Sine L, and Sethuraman G (1997) Relative efficacy of haloperidol and pimozide in children and adolescents with Tourette's disorder. *The American journal of psychiatry* **154:**1057-1062.

Shapiro E, Shapiro AK, Fulop G, Hubbard M, Mandeli J, Nordlie J, and Phillips RA (1989) Controlled study of haloperidol, pimozide and placebo for the treatment of Gilles de la Tourette's syndrome. *Archives of general psychiatry* **46:**722-730.

Vrana M, Whittington D, Nautiyal V, and Prasad B (2017) Database of Optimized Proteomic Quantitative Methods for Human Drug Disposition-Related Proteins for Applications in Physiologically Based Pharmacokinetic Modeling. *CPT: pharmacometrics & systems pharmacology* **6:**267-276.

Yoo HK, Lee JS, Paik KW, Choi SH, Yoon SJ, Kim JE, and Hong JP (2011) Open-label study comparing the efficacy and tolerability of aripiprazole and haloperidol in the treatment of pediatric tic disorders. *European child & adolescent psychiatry* **20:**127-135.

Zhou SF, Xue CC, Yu XQ, Li C, and Wang G (2007) Clinically important drug interactions potentially involving mechanism-based inhibition of cytochrome P450 3A4 and the role of therapeutic drug monitoring. *Therapeutic drug monitoring* **29:**687-710.

Footnotes

This work was funded by the National Institutes of Health (NIH) [Grant 1 U54 HD090258] "Genomic- and Ontogeny-Linked Dose Individualization and cLinical Optimization for Kids". BDC is supported by the NIH grant [T32 HD069038] "Research Fellowship Program in Pediatric Clinical/Developmental Pharmacology".

Legends for Figures

Figure 1. Elution of hydroxypimozide isomers and DHPBI with products of CYP2D6- and CYP3A4-mediated metabolism. Chromatograms for combined standards of 50 nM DHPBI (*m/z* 218.10 → 84.00) **(A)** and 5-/6-hydroxypimozide metabolites (*m/z* 478.30 → 328.10) **(B)** are provided for reference. Chromatograms from incubations of therapeutically relevant concentrations (10 nM) of pimozide in 2 pmol/mL recombinant CYP2D6: *m/z* 218.10 → 84.00 **(C)** and *m/z* 478.30 → 328.10 **(D),** and CYP3A4, *m/z* 218.10 → 84.00 **(E)** and *m/z* 478.30 → 328.10 **(F)** are also displayed. Retention times are listed in blue above the respective peaks.

Figure 2. Kinetics of pimozide biotransformation to DHPBI and 5-hydroxypimozide by recombinant CYP3A4 (left) and CYP2D6 (right) respectively. The displayed results are from a representative experiment. Individual data points represent the mean of technical duplicates at a given pimozide concentration from the same experimental replicate and the solid line reflects the fit of a single-enzyme Michaelis-Menten model to the data. Mean ± SD for parameter (K_m and V_{max}) estimates from n = 3 experiments using each isoform appear as text at the top of the respective graphs.

Figure 3. Kinetics of pimozide biotransformation to DHPBI (left) and 5-hydroxypimozide (right) in pooled human liver microsomes. The displayed results are from a representative experiment. Individual data points represent the mean of technical duplicates at a given pimozide concentration from the same experimental replicate and the solid line reflects the fit of a single-

enzyme Michaelis-Menten model to the data. Mean ± SD for parameter (K_m and V_{max}) estimates from n = 3 experiments appear as text at the bottom of the respective graphs for each reaction.

Figure 4. Correlation of CYP2D6 protein abundance and the rate of pimozide 5-hydroxylation (left) and pimozide 6-hydroxylation (right) in HLMs isolated from individual donors (n = 7). Data points represent the mean of separate experiments (n = 3) and error bars reflect the SD; error bars are not visible for many points due to low inter-experimental variability. The r^2 corresponding to the fit of a simple linear regression model for each metabolite is listed at the top of each respective graph. Expression of CYP2D6 protein was determined via MS/MS analysis. Data points were color coded to reflect activity score assignments for *CYP2D6* genotypes: 0 (red), 0.5 (yellow), 1.0 (green), 2.0 (blue) and >2.25 (purple) (Caudle et al., 2020).

Figure 5. Correlation of CYP3A4 protein abundance and the rate of pimozide N-dealkylation to DHPBI in HLMs isolated from individual donors (n = 7). Data points represent the mean of separate experiments (n = 3) and error bars reflect the SD; error bars are not visible for most points due to low inter-experimental variability. The r^2 corresponding to the fit of a simple linear regression model for each metabolite is listed at the top of each respective graph. Expression of CYP3A4 protein was determined via MS/MS analysis.

Figure 6. Revised pathway of pimozide biotransformation. The principle products of CYP2D6-mediated pimozide metabolism are 5- and 6-hydroxypimozide and the major product of CYP3A4-mediated metabolism of pimozide is DHPBI. Pimozide and metabolite structures were made using ChemDoodle Web Components 2D Sketcher (iChemLabs, Chesterfield, VA).

DMD Fast Forward. Published on August 26, 2020 as DOI: 10.1124/dmd.120.000188
This article has not been copyedited and formatted. The final version may differ from this version.

Tables

Table 1. Donor demographics, *CYP2D6* genotype and CYP protein content in single-donor HLMs

All single donor HLMs obtained for Sekisui Xenotech (Kansas City, KS). Activity scores were assigned according to the Clinical Pharmacogenetics Implementation Consortium (CPIC) guidelines (Caudle et al., 2020). Protein abundances for CYP2D6 and CYP3A4 were determined via MS/MS analysis.

Donor Product no.	Lot no.	Sex	Age (years)	*CYP2D6* Genotype	*CYP2D6* Activity Score	CYP2D6 (pmol/mg HLM protein)	CYP3A4 (pmol/mg HLM protein)
H0289	0710505	F	60	*1/*2x2*	>2.25[a]	11.93	71.71
H0439	0710037	F	78	**1/*4*	1.0[c]	3.31	4.97
H0446	0710044	M	21	**4/*41*	0.5[c]	0.80	48.85
H0455	0710053	F	37	**1/*4*	1.0[c]	4.25	35.53
H0485	0710139	M	10	**1/*2*	2.0[b]	4.20	2.41
H0486	0710140	F	49	**4/*5*	0.0[d]	<LOQ	44.44
H0493	0710147	F	64	**1/*1*	2.0[b]	7.49	34.94

[a] Ultra rapid metabolizer status predicted

[b] Normal metabolizer status predicted

[c] Intermediate metabolizer status predicted

[d] Poor metabolizer status predicted

Table 2. Molar balance of pimozide metabolism in pooled HLMs.

Mean (SD) amounts (pmol) of pimozide molecules depleted and pimozide metabolites formed by pooled (n = 200 donors) human liver microsomes incubated with pimozide (10 pmol starting amount, 50 nM starting concentration) for 20 min. Percentage standardization of metabolites formed relative to pimozide molecules depleted is also provided.

	5-Hydroxypimozide	6-Hydroxypimozide	DHPBI	Sum of Metabolites[a]	Pimozide Depleted[b]
Amount (pmol)	0.27 (0.040)	0.11 (0.035)	2.4 (0.20)	2.8 (0.17)	3.1 (0.80)
% Depleted Accounted[c]	8.7 (1.3)	3.5 (1.1)	78 (6.5)	90 (5.5)	*N/A*

[a] Denotes sum of amounts of DHPBI, 5-hydroxypimozide and 6-hydroxypimozide formed during each incubation.

[b] Denotes the difference between pimozide amounts measured at time 0 min and 20 min in each incubation.

[c] Sum of metabolite amounts divided by amount of pimozide depleted over the course of the incubation, expressed as a percentage (see Equation 1).

Table 3. Comparison of pimozide metabolite concentrations produced in incubations of recombinant CYP isoforms

Recombinant human cytochrome P450 isoforms (2 pmol/mL) were incubated with 2500 nM pimozide for 30 min. Numbers represent the mean (SD) from triplicate experiments for the concentrations (nM) of the specific metabolites observed following quenching of incubations. A "-" denotes a CYP isoform that was not observed to produce detectable amounts of the listed metabolites. The lower LOQs for this experiment was 1 nM for 5-/6-hydroxypimozide and 5 nM for DHPBI. Experimental conditions were not confirmed to be linear with respect to time.

Cytochrome P450 Isoform	1A1	1A2	2A6	2B6	2C8	2C9	2C18	2C19	2D6	2E1	2J2	3A4	3A5	3A7
DHPBI	-	-	-	-	-	-	-	-	-	-	-	78 (6.5)	< LOQ	14 (1.5)
5-OH-Pimozide	< LOQ	< LOQ	-	-	-	-	< LOQ	-	35 (11)	-	< LOQ	2.4 (0.24)	2.5 (0.22)	< LOQ
6-OH-Pimozide	< LOQ	< LOQ	-	-	-	-	< LOQ	-	5.8 (1.2)	-	< LOQ	1.7 (0.33)	1.4 (0.16)	< LOQ

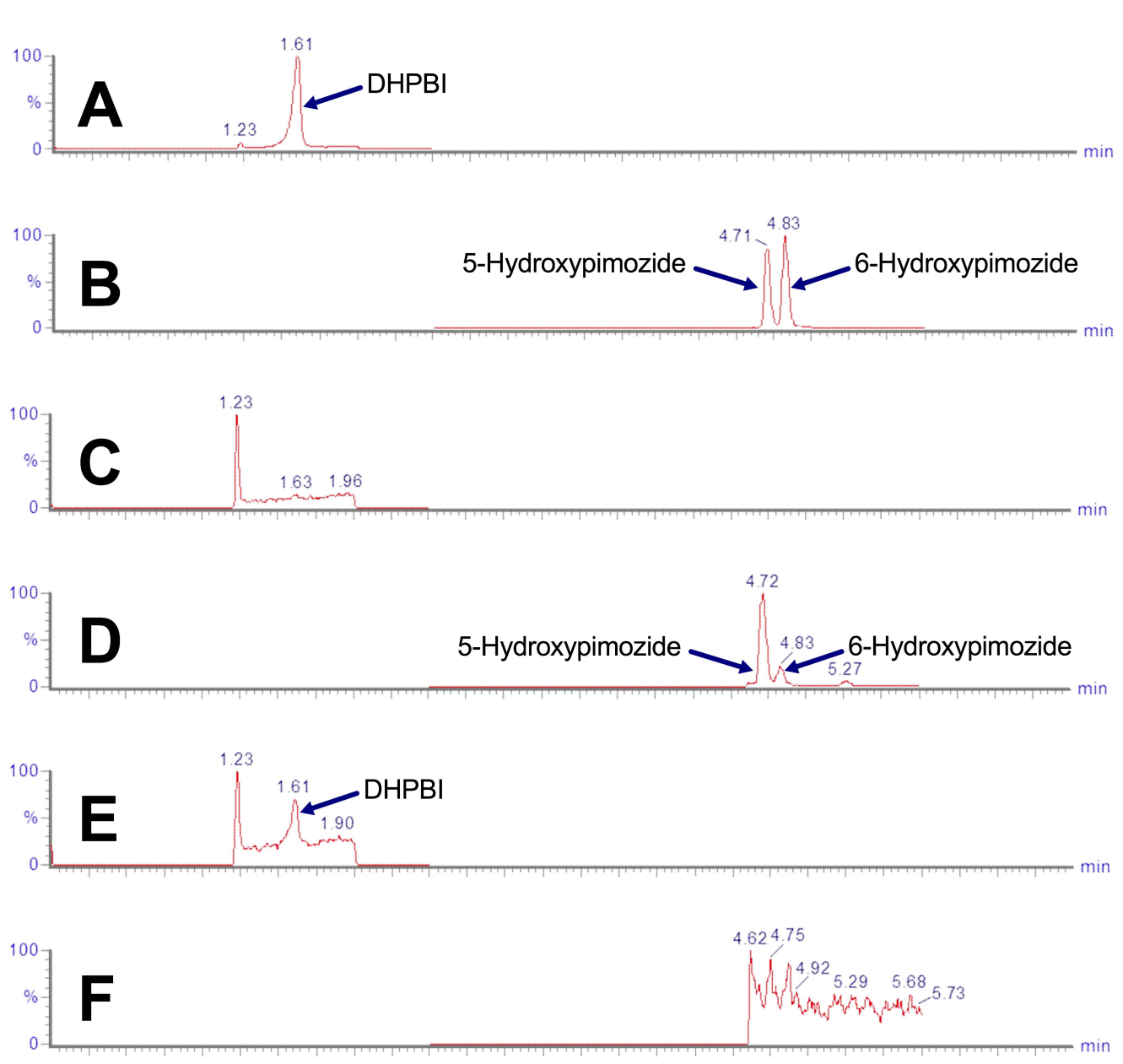
A
1.61
DHPBI
1.23
B
4.71
4.83
5-Hydroxypimozide
6-Hydroxypimozide
C
1.23
1.63
1.96
D
4.72
5-Hydroxypimozide
4.83
6-Hydroxypimozide
5.27
E
1.23
1.61
DHPBI
1.90
F
4.62
4.75
4.92
5.29
5.68
5.73
100
%
0
min

Figure 1

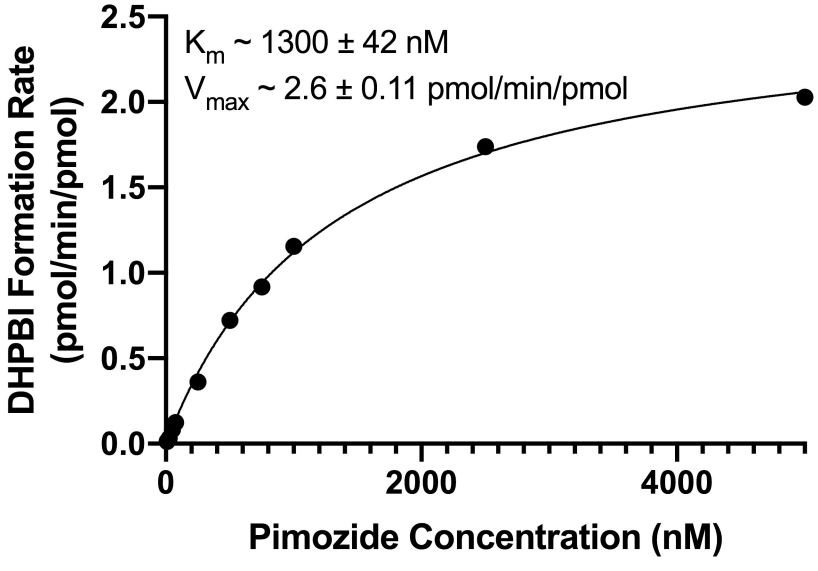

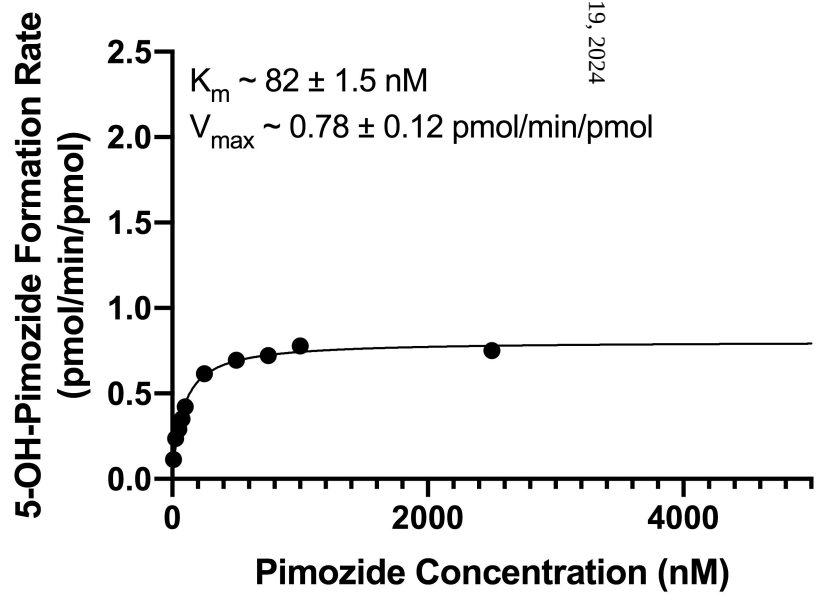

Figure 2

DMD Fast Forward. Published on August 26, 2020 as DOI: 10.1124/dmd.120.000188
This article has not been copyedited and formatted. The final version may differ from this version.

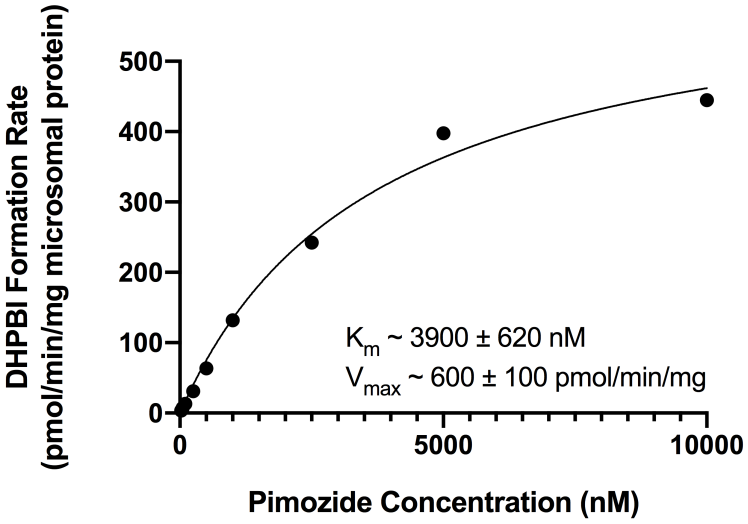

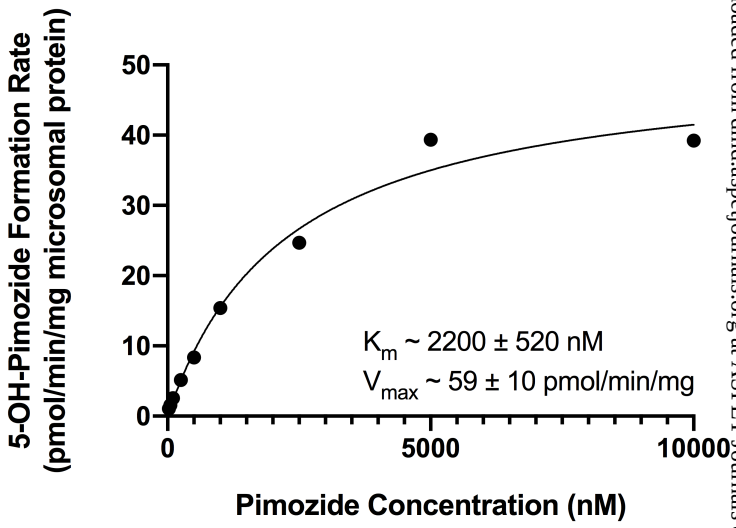

Figure 3

DMD Fast Forward. Published on August 26, 2020 as DOI: 10.1124/dmd.120.000188
This article has not been copyedited and formatted. The final version may differ from this version.

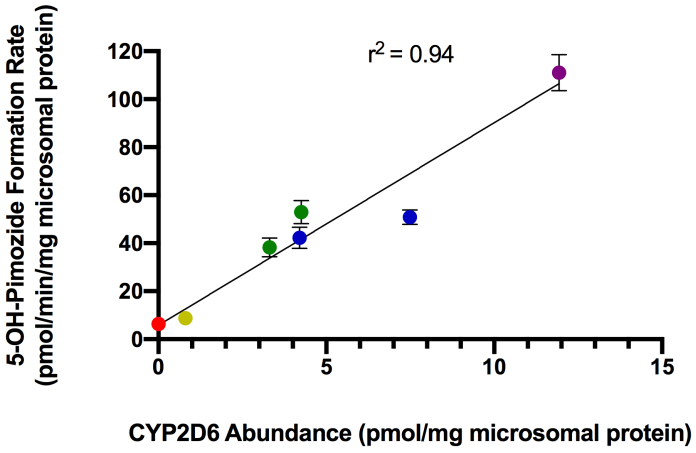

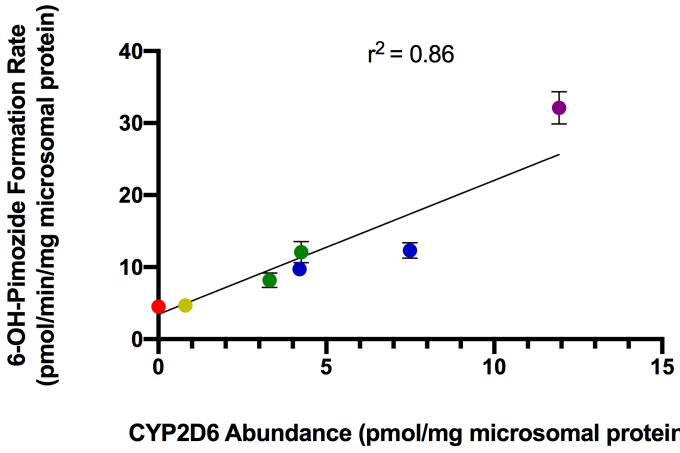

Figure 4

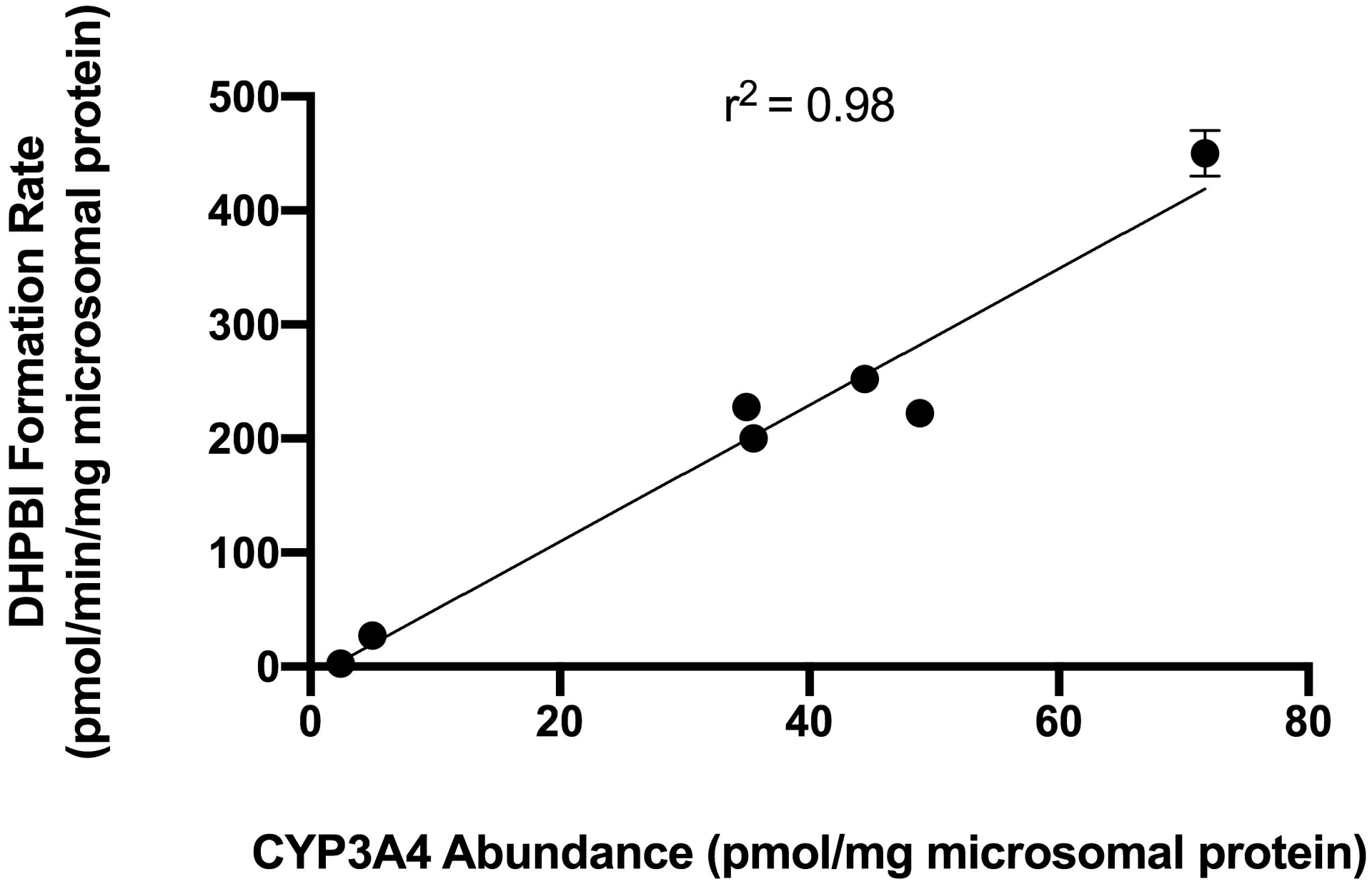
DHPBI Formation Rate
(pmol/min/mg microsomal protein)
500
400
300
200
100
0
r^2 = 0.98
0
20
40
60
80
CYP3A4 Abundance (pmol/mg microsomal protein)

Figure 5

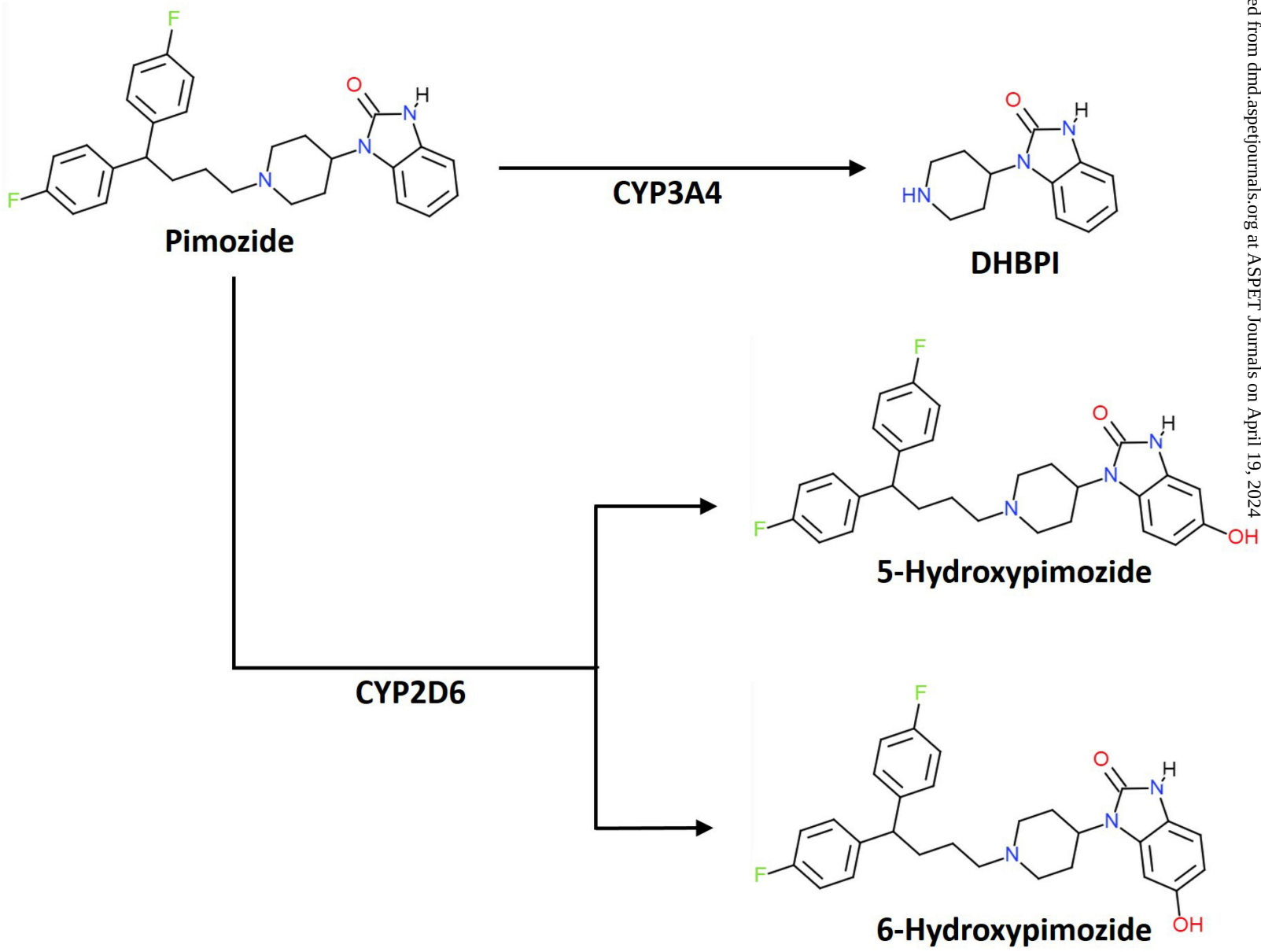

Figure 6